Journal of Soft Computing in Civil Engineering 7-2 (2023) 155-175

Contents lists available at SCCE

Journal of Soft Computing in Civil Engineering

Journal homepage: www.jsoftcivil.com

Comparison of DEEP-LSTM and MLP Models in Estimation of Evaporation Pan for Arid Regions

Amirhossein Samii[1], Hojat Karami[2*], Hamidreza Ghazvinian[2], Amirsaeed Safari[3*], Yashar Dadras Ajirlou[2*]

1. Advanced Robotics and Automated Systems (ARAS), Faculty of Electrical Engineering. K. N. Toosi University of Technology, Tehran, Iran
2. Department of Water Engineering and Hydraulic Structures, Faculty of Civil Engineering, Semnan University, Semnan, Iran
3. Ph.D. Student, Department of Mechanical Engineering, University of Kentucky, Lexington, KY, United States

Corresponding author: *hkarami@semnan.ac.ir*

https://doi.org/10.22115/SCCE.2023.367948.1550

ARTICLE INFO

Article history:
Received: 31 October 2022
Revised: 17 January 2023
Accepted: 31 January 2023

Keywords:
Evaporation pan;
DEEP-LSTM;
MLP;
Meteorological data;
Semnan;
Garmsar.

ABSTRACT

The importance of evaporation estimation in water resources and agricultural studies is undeniable. Evaporation pans (EP) are used as an indicator to determine the evaporation of lakes and reservoirs around the world due to the ease of interpreting its data. The purpose of this study is to evaluate the efficiency of the Long-Short Term Memory (LSTM) model to estimate evaporation from a pan and compare it with the Multilayer Perceptron (MLP) model in Semnan and Garmsar. For this purpose, daily meteorological data recorded between 2000 and 2018 (19 consecutive years) in Semnan and Garmsar synoptic stations were used. Minimum and maximum air temperature (Tmax, Tmin), wind speed (WS), sunshine hours (SH), air pressure (PA), relative humidity (RH) were selected as input data and evaporation data from the pan (EP) was considered as the output of the case. Also, in modeling both networks in the input section, 4 different scenarios were used. The two studied models were evaluated by the evaluation criteria of coefficient of determination (R^2), root mean square error (RMSE) and mean absolute error (MAE). The results showed that among the studied scenarios, the fourth scenario (considering all input parameters) had the highest R^2 and the lowest RMSE and MAE. In general, the two models performed well in predicting the rate of evaporation. Also, in both stations, the LSTM model had more R^2 and less RMSE and MAE than the MLP model. The values of R^2, RMSE and MAE for the best DEEP-LSTM model (LSTM4) for Semnan city were 0.9451, 1.8345 and 0.5437 and for Garmsar city 0.9204, 1.8323 and 1.3531 respectively.

How to cite this article: Samii A, Karami H, Ghazvinian H, Safari A, Dadrasajirlou Y. Comparison of DEEP-LSTM and MLP models in estimation of evaporation pan for arid regions. J Soft Comput Civ Eng 2023;7(2):155–175. https://doi.org/10.22115/scce.2023.367948.1550

1. Introduction

In recent years, climate changes and increasing water demand have caused problems in the sustainable management of water resources in the country [1]. This is especially important in the case of drinking water supply, and sometimes it has caused a tendency to supply different water needs from underground water sources and an excessive drop in the level of some aquifers in the country [2,3]. On the other hand, every year, millions of cubic meters of fresh water stored behind the dams, which are built and maintained at huge costs, evaporate and are wasted [4].

Accurate and timely estimation of evaporation has a significant and vital impact on preserving water resources and agriculture and hydrology, which is used to estimate the water required by crops for irrigation planning and drought management [5]. Evaporation is a critical phenomenon in hydrological studies which understanding its amount is vital for management of irrigation systems and water resources [6–8]. One method of estimating evaporation is using evaporation pans [9–14], which is well-known as a means of measuring evaporation from the free surface of water globally [15,16]. Given the importance of evaporation and its high impact on climate change and the amount of freshwater resources that lead to negative effects on water resources, accurate prediction of evaporation is essential in the hydrological cycle [17]. Many parameters affect the rate of evaporation, including relative humidity, temperature, wind speed, and sunshine hours [18–22]. Another method of predicting the rate of evaporation is the use of intelligent methods [23–26]. Intelligent methods have been welcomed due to the reduction of computation time, as well as the reduction of trial and error process [27,28].

In recent years, many intelligent models have been proposed to estimate the rate of evaporation, including the MLP model [12,13,29–31], SVR model [14,25,32–34], M5tree model [35–38], GEP model [35,39,40], ANFIS model [40–43]. Also, various hybrid models in evaporation simulation have been presented [12,23,30,41,44–46]. Table 1 provided some studies in connection with research on estimating the rate of evaporation by intelligent methods.

Due to the fact that very few studies have been conducted to estimate evaporation using deep learning methods, the purpose of this study was to compare the performance of two models of artificial neural network and Long- Short Term Memory (LSTM) to estimate evaporation from the pan in Semnan and Garmsar cities from Semnan province of Iran. Considering that the mentioned cities are in hot and dry weather conditions, in this research we seek to investigate the efficiency of LSTM model in predicting evaporation in dry areas. Also, the results of the LSTM model of the current research were compared with the results of other researches that estimate evaporation from the pan with soft computing model. Meteorological parameters of T_{min}, T_{max}, WS, SH, PA, RH and EP were examined as input data. The present study also answers the question whether the two ANN and LSTM models are suitable methods for estimating evaporation in the cities of Semnan and Garmsar?

2. Data and studied areas

Semnan province locates in northeastern of Iran (Figure 1), where its center is Semnan city [47]. The area of this province is 97491 Km^2 [48]. The cities of Semnan and Garmsar have arid and semi-arid climatic conditions. In this study, 19 consecutive years of daily meteorological data of synoptic stations of Semnan and Garmsar between 2000 and 2018 were considered. The data is equivalent to 6935 data, including minimum and maximum temperature, sunny hours, wind speed, air pressure, relative humidity and evaporation.

Table1
Summery of existing models.

Previous work	Number of years study	Station	Methods	R^2	Input variables
Kisi, 2015 [49]	20	Mersin	LLSVM	0.88	AT[1], SR[2], WS, RH, EP
			M5 Tree	0.76	
			MARS	0.86	
	20	Antalya	LLSVM	0.93	
			M5 Tree	0.92	
			MARS	0.88	
Wang et al., 2017 [38]	39	Yangtze River Basin IDs 57461	ANFIS-GP	0.93	AT, SR, PA, WS
			FG	0.93	
			M5Tree	0.91	
	39	Yangtze River Basin IDs 57494	ANFIS-GP	0.89	
			FG	0.90	
			M5Tree	0.90	
	39	Yangtze River Basin IDs 57516	ANFIS-GP	0.96	
			FG	0.97	
			M5Tree	0.95	
	39	Yangtze River Basin IDs 58238	ANFIS-GP	0.95	
			FG	0.95	
			M5Tree	0.92	
	39	Yangtze River Basin IDs 58321	ANFIS-GP	0.92	
			FG	0.90	
			M5Tree	0.90	
	39	Yangtze River Basin IDs 58362	ANFIS-GP	0.95	
			FG	0.95	
			M5Tree	0.92	
Malik et al., 2017 [50]	4	Himalayas, Uttarakhand	RBNN	0.87	T_{min}, T_{max}, $RH_{morning}$, $RH_{afternoon}$, WS, SH, EP
			SOMNN	0.83	
			MLR	0.81	
Eray et al., 2018 [51]	27	Antakya	MGGP	0.92	T_{min}, T_{max}, RA, RH, WS, EP
			GP	0.94	
			DENFIS	0.94	
	39	Antalya	MGGP	0.95	
			GP	0.95	
			DENFIS	0.93	
Moazenzadeh et al., 2018 [33]	10	Lahijan	SVR	0.78	T_{min}, T_{max}, RA, RH, WS, EP, P[3], SH
			SVR-FA	0.79	
	10	Rasht	SVR	0.74	
			SVR-FA	0.81	
Majhi et al., 2019 [52]	34	Raipur	Deep-LSTM	0.91	T_{min}, T_{max}, $RH_{morning}$, $RH_{afternoon}$, WS, SH, EP
			MLANN	0.88	
	24	Jagdalpur	Deep-LSTM	0.76	
			MLANN	0.76	
	16	Ambikapur	Deep-LSTM	0.71	
			MLANN	0.70	
Karami et al., 2021 [53]	9	Garmsar	GMDH-NN	0.84	T_{min}, T_{max}, WS, RH, PA, SH
Shahi et al., 2021 [54]	16	Dameghan	ANN	0.80	T_{min}, T_{max}, RH, WS,SH
Abed et al., 2021 [55]	19	Alor Setar	LSTM	0.97	T_{min}, T_{max}, RH, WS,, RA, SH
		Kota Bharu	LSTM	0.98	

[1] Air Temperature
[2] Solar Radiation
[3] Precipitation

The daily evaporation rate of the pan was modeled as a dependent variable and other parameters were modeled as independent variables. 70% of the data were used for training and 30% for data. 30% of the data is completely random and selected by the algorithm itself. This makes the inherited characteristic not transmitted by the time series and the ability to check the machine learning towards the reality. Table 2 provides the abbreviations of the six input data and one output data used in this study. Also the statistical specifications of input and output data [56]. For better data performance in both models, the input and output data were normalized using Equation (1). Thus, all data are formed between 0.1 and 0.9 and then used in relationship development [31,53].

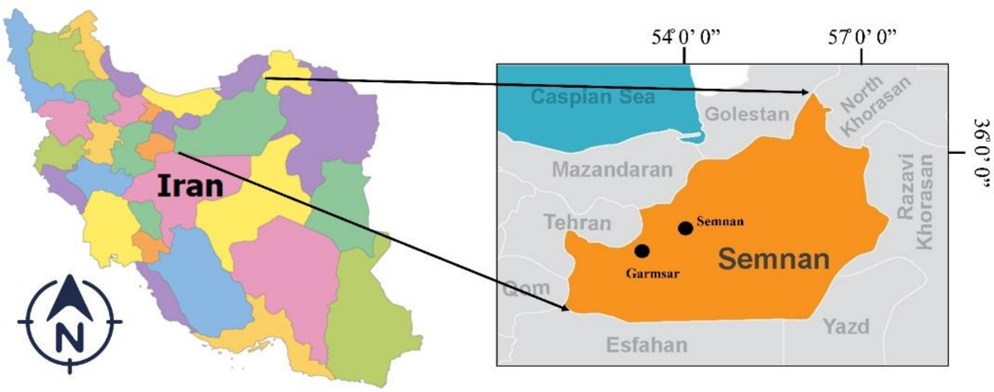

Fig. 1. Location of the study area.

Table 2
Statistical characteristics of input and output data.

Station	Dataset	Climatic data	Mean	Minimum	Maximum	Standard deviation
Semnan	Tmax(°c)	Maximum temperature	29.51	3.8	43.8	8.37
	Tmin(°c)	Minimum temperature	17.64	-1.6	33	7.55
	SH(Hours)	Sunshine hours	9.36	0.00	14.2	2.98
	WS(m/s)	Wind speed	6.49	0.00	22	3.03
	PA(hPa)	Air pressure	886.62	872.53	902.70	4.58
	RH (%)	Relative humidity	31.16	6.50	91.5	15.59
	EP (mm)	Evaporation	9.11	0.00	25	4.92
Garmsar	Tmax(°c)	Maximum temperature	26.31	-1.6	47	9.71
	Tmin(°c)	Minimum temperature	13.08	-1.2	35	11.08
	SH(Hours)	Sunshine hours	8.79	0.00	13.8	3.27
	WS(m/s)	Wind speed	7.27	0.00	35	3.99
	PA(hPa)	Air pressure	914.71	887.8	936.98	12.58
	RH (%)	Relative humidity	37.13	4.5	97.6	19.34
	EP (mm)	Evaporation	7.37	0.00	39.1	6.69

$$Parameter_{Scaled} = \left[(0.9-0.1)\left(\frac{Parameter - Parameter_{\min}}{Parameter_{\max} - Parameter_{\min}} \right) \right] + 0.1 \tag{1}$$

One method for measuring evaporation is using different evaporation pans. One of the most common types of pans is used in synoptic and meteorological stations is the Class A pan. In

Semnan and Garmsar synoptic stations, evaporation data were collected using this type of pan. Evaporation pans are made of galvanized iron or stainless steel with a thickness of 1.5 mm in a circle shape with a standard diameter (48 inches) and a height of 25.4 cm (10 inches). The bottom of the pan is integrated and its upper edges have a resistant fold. The water depth is 20 cm. Class A pans are usually placed on pedestals made of wood. The height of these bases is 15 cm from the ground. Figure 2 shows a graphical view of a standard Class A evaporator.

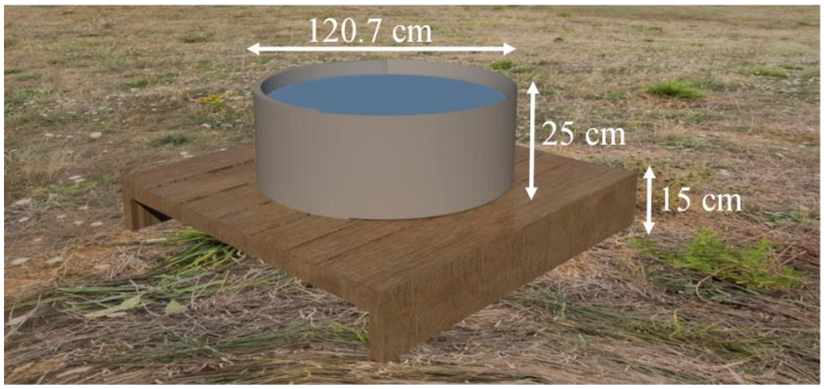

Fig. 2. Standard Class A Evaporation Pan.

3. Multilayer perceptron network (MLP)

The Multilayer Perceptron network [57,58] is a forward neural network that consists of input (first layer), hidden (second layer) and output (third layer)[59]. The purpose of training this network is to achieve generalizability and learning, this means that the network is able to correctly identify patterns that it has not seen in the training phase, as well as correctly identify training patterns [60]. The training of this network is done in two stages, forward and backward which means that the data moves toward the output layer and after calculation of the error, the error comes back to the input layer [61]. The structure of this network is shown in Figure 3. In this study, the number of input data was 3, 4, 5 and 6. The number of neurons in the secretory and output layers are 5 and 1, respectively. Hyperbolic tangent (tanh) was used as the activation function.

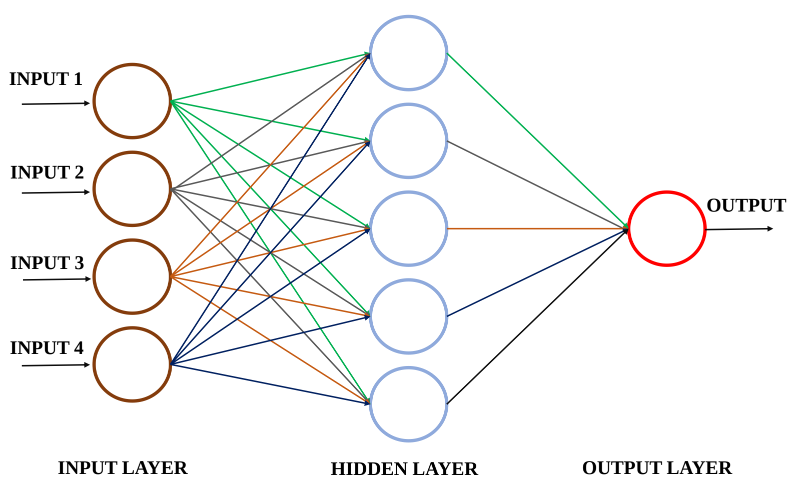

Fig. 3. An artificial neural network with 3 layer.

4. Long short term memory (LSTM)

LSTM is a recursive neural network architecture designed to store and access information better than the traditional version. The unit of LSTM was first introduced by Hochreiter and Schmidhuber (1997). The LSTM network uses a Ct memory at time t. ht is expressed as the output or activation of the LSTM unit. Γ_0 is the output gateway that controls the amount of content delivered through memory [63]. σ is the Softmax activation function. W0 is also an hermitian matrix. The Ct memory cell is also the current memory with relative forgetfulness. New memory content is obtained with the expression C [63]. The amount of current memory to be forgotten is controlled by the bf forgetfulness gateway, and the amount of new memory to be added to the memory cell is updated by the gateway. Improved versions, such as LSTM, show that this capability is provided to the network by imposing restrictions on the freedom of parameters (by inserting new gateways) in the optimization process. Figure 4 shows an LSTM network. Equations 2 to 7 are provided for the network. In this study, LSTM layer nodes, Dense layer-1 nodes, Dense layer-2 nodes, Batch size and Epoch were considered 32, 20, 20, 72 and 300, respectively.

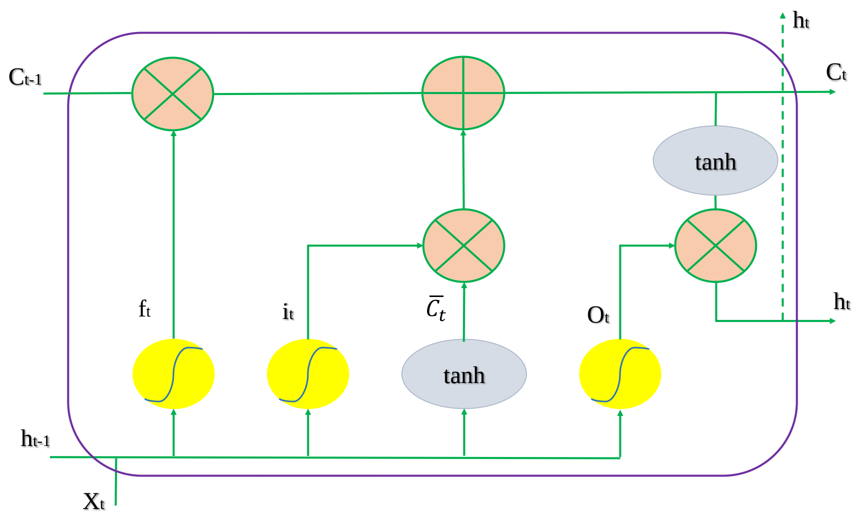

Fig. 4. Internal structure of an LSTM block.

$$\hat{C} = \tanh(W_C \cdot [h_{t-1}, X_t] + b_c) \quad (2)$$

$$C_t = \Gamma_f = \sigma(W_f \cdot [h_{t-1}, X_t] + b_f) \quad (3)$$

$$\Gamma_f = \sigma(W_f \cdot [h_{t-1}, X_t] + b_f) \quad (4)$$

$$\Gamma_u = \sigma(W_u \cdot [h_{t-1}, X_t] + b_u) \quad (5)$$

$$\Gamma_o = \sigma(W_o \cdot [h_{t-1}, X_t] + b_o) \quad (6)$$

$$h_t = \Gamma_o . \tanh(C_t) \quad (7)$$

5. Evaluation criteria

Explanation coefficient (R^2)[64,65], root mean square error (RMSE)[66] and mean absolute error (MAE)[67] were used to evaluate the performance of the models [68]. Equations 8 to 10 represent R^2, RMSE, and MAE, respectively. The closer the R^2 is to one, the higher the correspondence between the observational data and the modeling data. The closer the MAE and RMSE indices are to zero, the better the matching of the observed and simulated data.

$$R^2 = \left[\frac{\sum_{i=1}^{n} (x_i - \bar{x})(y_i - \bar{y})}{\sum_{i=1}^{n} (x_i - \bar{x})^2 \sum_{i=1}^{n} (y_i - \bar{y})^2} \right] \tag{8}$$

$$RMSE = \sqrt{\frac{\sum_{i=1}^{n} (y_i - x_i)^2}{N}} \tag{9}$$

$$MAE = \frac{1}{N} \sum_{i=1}^{n} \left| (y_i - x_i) \right| \tag{10}$$

In equations 8 to 10, x_i is the observational evaporation value at the station, y_i is the simulated evaporation value, $\bar{x}$ is the mean observational evaporation value at the station, and $\bar{y}$ is the equivalent average for the simulated values.

6. Result and discussion

To estimate daily evaporation, LSTM and MLP models are simulated in Python. Different input combinations for the two models are shown in Table 3. The lowest input is for the first combination. Which contains only three parameters of minimum temperature, maximum temperature, and relative humidity. In input combination No. 4, all data is used as input for modeling. The different combinations of input parameters are to check the effectiveness and efficiency of each meteorological data on evaporation in the study areas .In fact, by considering different combinations of input data and removing one or more parameters in a combination, the effect of that parameter on evaporation can be identified .Also, this method can show whether more accurate simulation results are obtained by having more input data.

Table 3
Input combination used in modeling.

scenario	Models	Input combination	Number of input
1	LSTM1 & MLP1	T_{max}, $T_{min,}$ RH	3
2	LSTM2 & MLP2	T_{max}, $T_{min,}$ RH, WS	4
3	LSTM3 & MLP3	T_{max}, $T_{min,}$ RH, WS, SH	5
4	LSTM4 & MLP4	T_{max}, $T_{min,}$ RH, WS, SH , PA	6

The performance of the proposed models based on the evaluation criteria is shown in Table 4. Overally, scenario 4 was superior for both stations and for both LSTM and MLP models. The best model for both stations is the LSTM4 model. Considering the performance of LSTM4 for Semnan station, the values of R^2, RMSE and MAE were estimated 0.9451, 1.8345, 0.5437 respectively, where their values for Garmsar station are 0.9255, 1.7920 and 1.3513, respectively. In total, the value of R^2 for all inputs in both models is higher than 0.9, which indicates the proper performance of both models. Comparing the LSTM and MLP models in pairs, the results show that LSTM has a better performance than MLP in both stations. This obtained result is consistent with Majhi et al. [52]. The best prediction accuracy was obtained with models that used the complete meteorological data set for both stations. This showed that the prediction accuracy of the model increases with having more input parameters, which is consistent with the studies of Wang et al. [69] and Fan et al. [70].

Abed et al. [55] used minimum temperature, maximum temperature, average temperature, wind speed, relative humidity and solar radiation data as input to estimate the evaporation rate using XGB, Elastic Net LR and LSTM models. Also Majhi et al. [52] have used minimum and maximum temperature, morning and afternoon relative humidity, wind speed and solar radiation data as input for LSTM and MLP models. Best results for both above research are obtained when all the input data were considered into the estimation process. The results of Qasem et al. [14] also showed that the higher the number and types of inputs, the higher the accuracy of the results by ANN, WANN, SVR and WSVR models. Alsumaiei [71] used the ANN for the dry area of Kuwait International Airport (KIA) to model the evaporation rate, the results of which are consistent with the obtained results in current study. Figures 5 and 6 show the time series of the observed and simulated data of daily evaporation from the pan for Semnan and Garmsar stations, respectively. In other words, these figures are a comparison of total observational and simulated data for LSTM and MLP models. The more the simulated values correspond to the measured values, the more accurate and less error the model will have. In LSTM4 and MLP4 there is less visual difference between the observed and simulated data. Also, this difference for Garmsar station is less than Semnan station. The scattering curve of the estimated values against the observed values for both training and testing and for both Semnan and Garmsar stations can be seen in Figures 7 and 8, respectively. In Singh et al. [21] a comparison between machine learning and ANN and statistical technique versus MLR to predict pan evaporation found that the correlation coefficient of SVR and ANN was higher than the MLR model for calibration and validation.

In Alsumaiei [71], it was stated that the MLP model can have a relatively good performance in predicting evaporation in arid and very arid regions, which is confirmed by the results obtained in the present study. Majhi et al. [52] and Abed et al. [55] show that the LSTM model can have high efficiency in estimating and modeling the rate of evaporation from the pan in humid and very humid climates. The current study showed that the DEEP-LSTM model for hot and dry areas has a good performance in estimating evaporation from the pan, which is in line with the results of Majhi et al. [52] and Abed et al. [55].

Table 4
Comparison of performance of LSTM and MLP models in estimating evaporation of Semnan and Garmsar stations.

Station	Models	R^2	RMSE	MAE
Semnan	LSTM1	0.9315	1.8923	1.059
	MLP1	0.9004	2.1036	1.0395
	LSTM2	0.9320	1.8887	1.0845
	MLP2	0.9272	1.9227	1.0641
	LSTM3	0.9359	1.8605	1.1202
	MLP3	0.9348	1.8613	1.1230
	LSTM4	0.9451	1.8345	0.5437
	MLP4	0.9395	1.8544	1.1329
Garmsar	LSTM1	0.9080	1.9291	1.2402
	MLP1	0.9078	1.9301	1.2671
	LSTM2	0.9115	1.9018	1.2524
	MLP2	0.9100	1.9133	1.2530
	LSTM3	0.9170	1.8564	1.3420
	MLP3	0.9111	1.9055	1.3312
	LSTM4	0.9255	1.7920	1.3513
	MLP4	0.9204	1.8323	1.3531

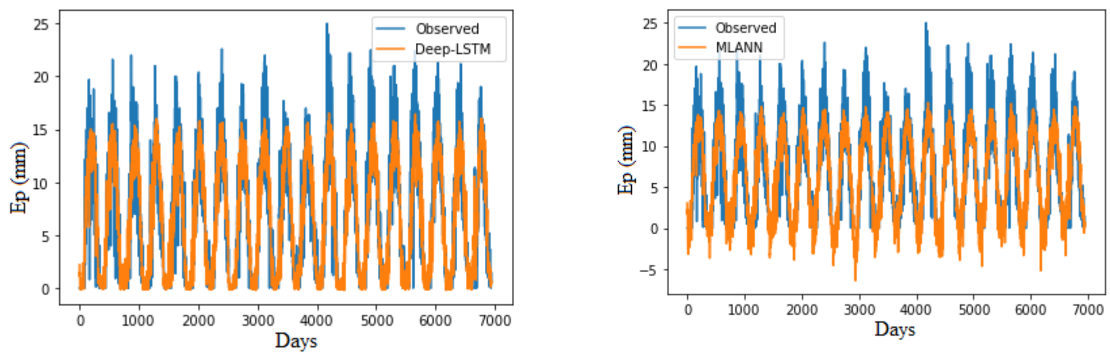

a b

Fig. 5. Time series of observed and simulated values with LSTM and MLP models for Semnan station, a and b (scenario 4).

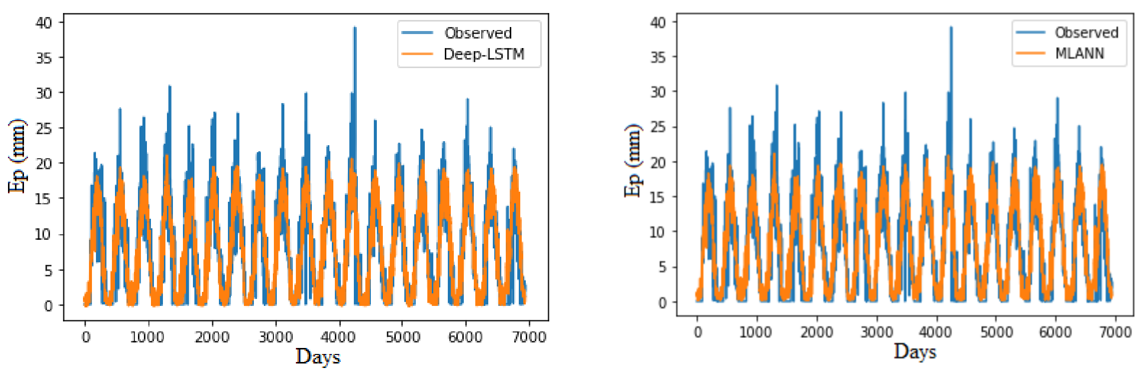

a b

Fig. 6. Time series of observed and simulated values with LSTM and MLP models for Garmsar station, a and b (scenario 4).

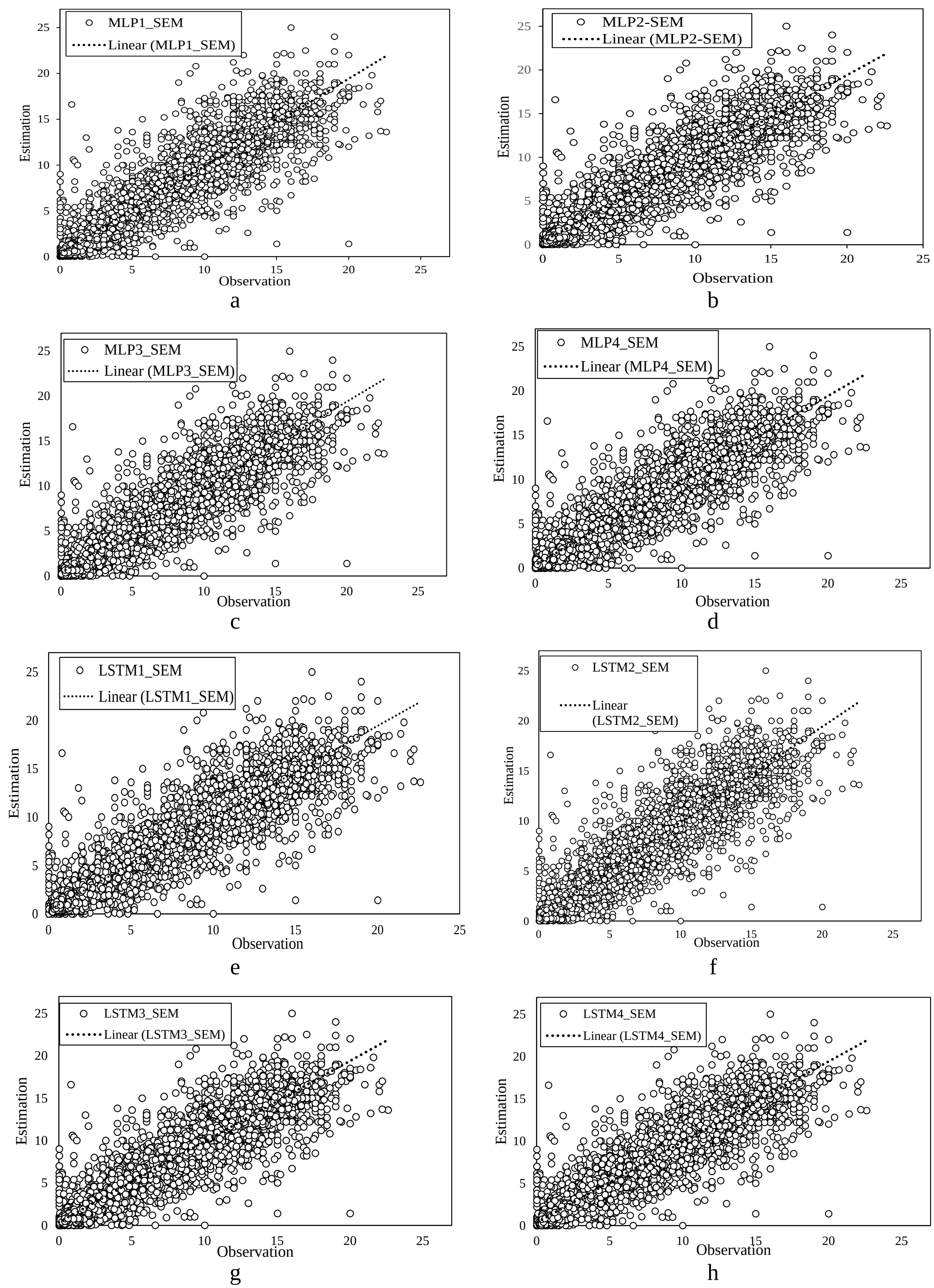

Fig. 7. Comparison of experimental results and simulation results of Semnan station pan evaporation, a to: d MLP model and e to h: LSTM model.

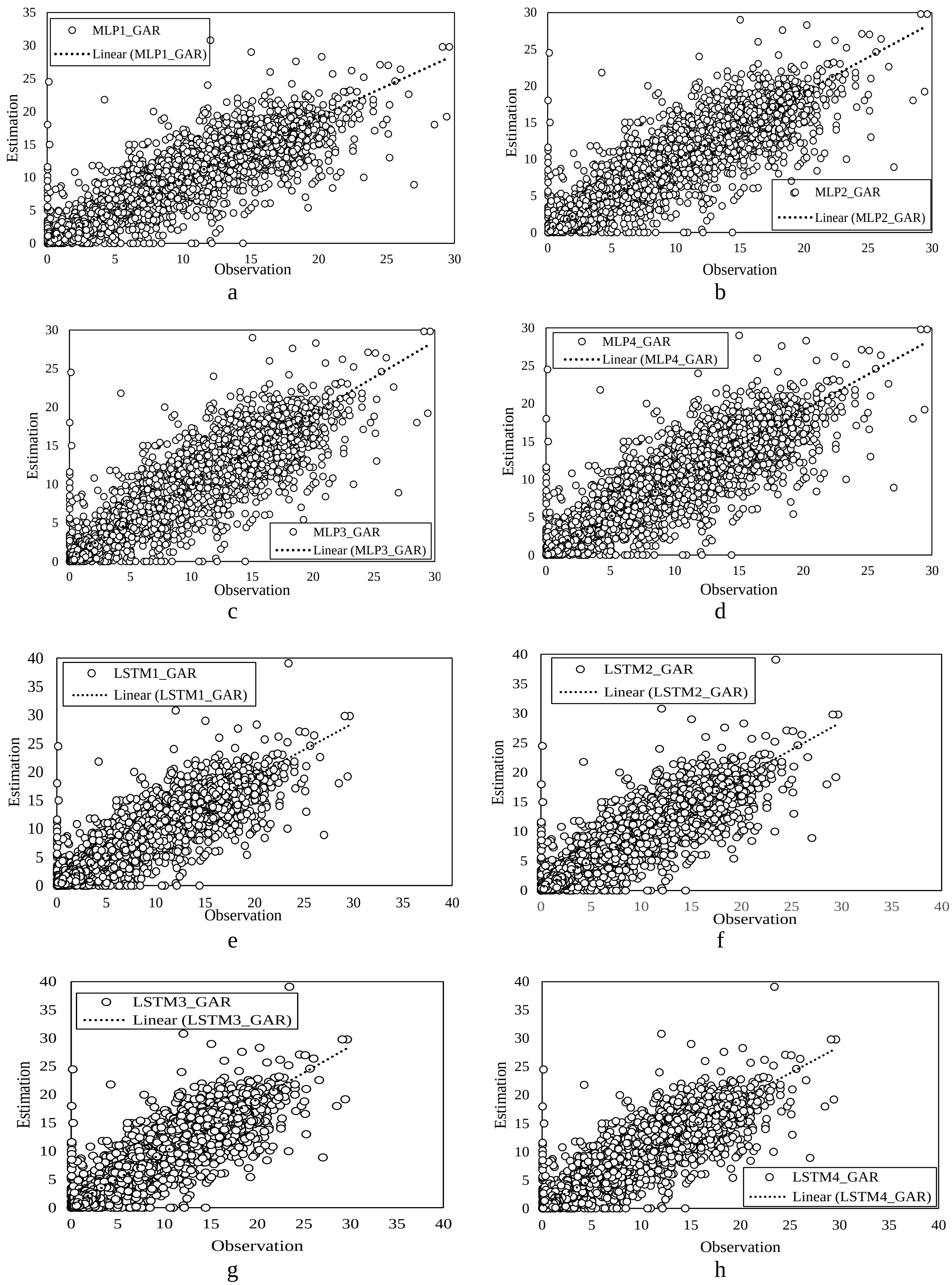

Fig. 8. Comparison of experimental results and simulation results of Gharmsar station pan evaporation, a to: d MLP model and e to h: LSTM model.

A radar chart is a graph that shows the status of various required variables by displaying one or more polygons. By looking at the radar chart, the degree of proximity and similarity of the same variables will be understood. One of the main applications of radar charts is to compare observational status with predicted status considering some criteria. Figure 9 shows the radar diagrams of LSTM and MLP models for different scenarios in Semnan and Garmsar stations. Based on these graphs, both models performed well in both stations in terms of R^2, RMSE and MAE evaluation criteria, and the LSTM4 performed better for both stations. These results are in good agreement with the research of Yin et al. [72] and Ferreira and Da Cuna [73].

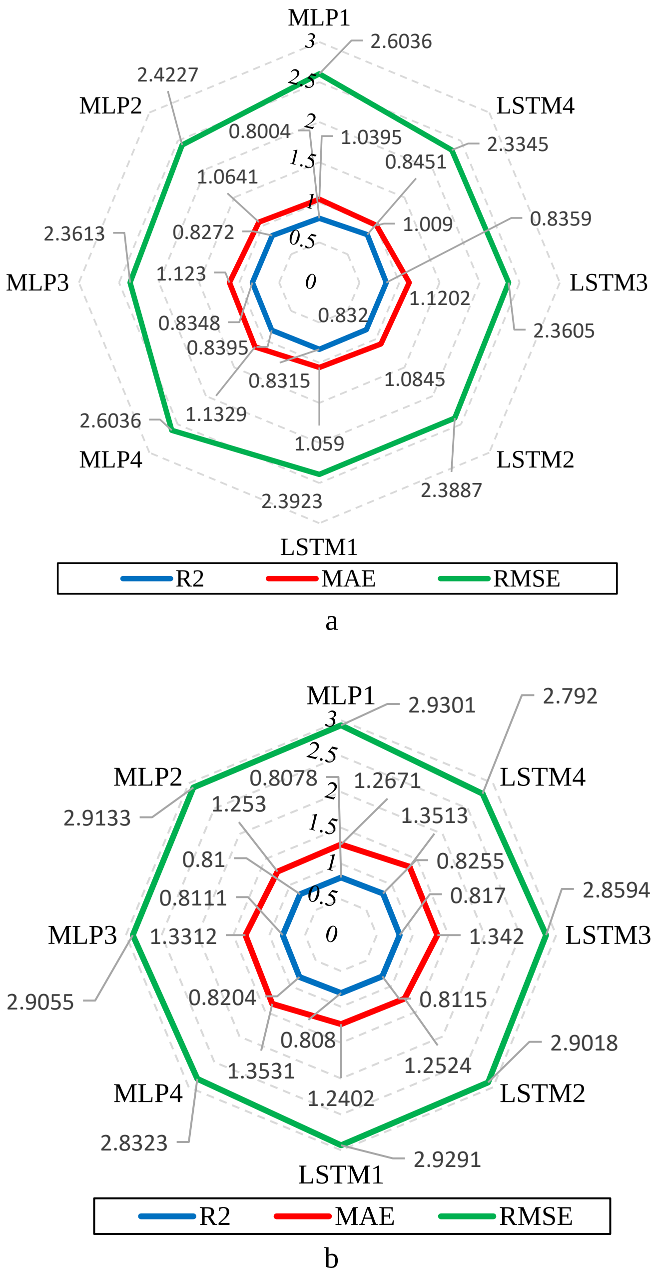

Fig. 9. Radar diagram of LSTM and MLP models a: Semnan and b: Garmsar.

The box diagram of the results obtained in the test phase for Semnan and Garmsar stations are shown in Figures 10 and 11. The middle line shows the difference between the average observed values and the estimated average daily evaporation values in millimeters. The first line and the last line of the boxes show the 25th and 75th percentiles respectively, and the line in the middle of the box shows the average.

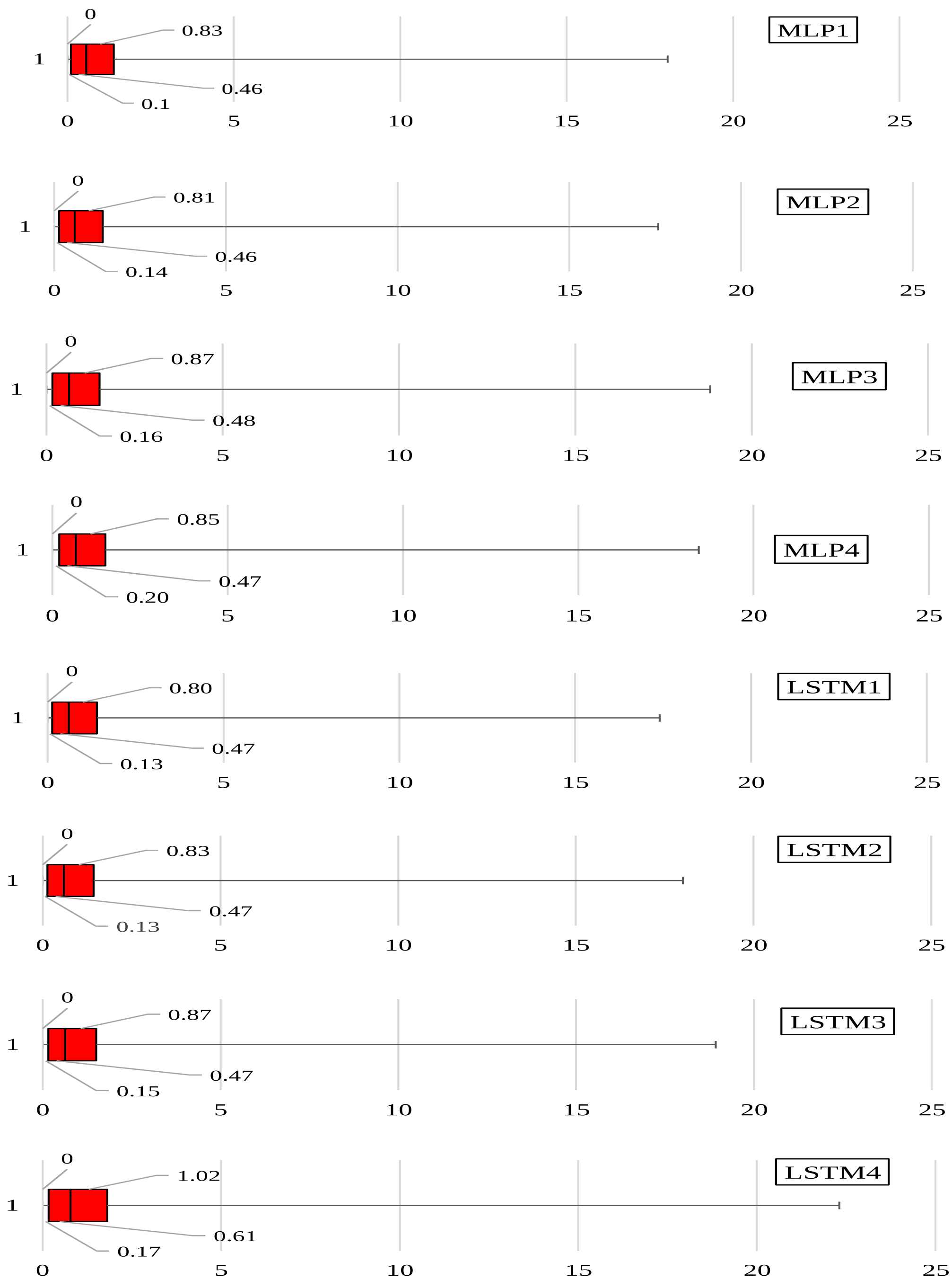

Fig. 10. Box diagram of MLP and LSTM models for Semnan station.

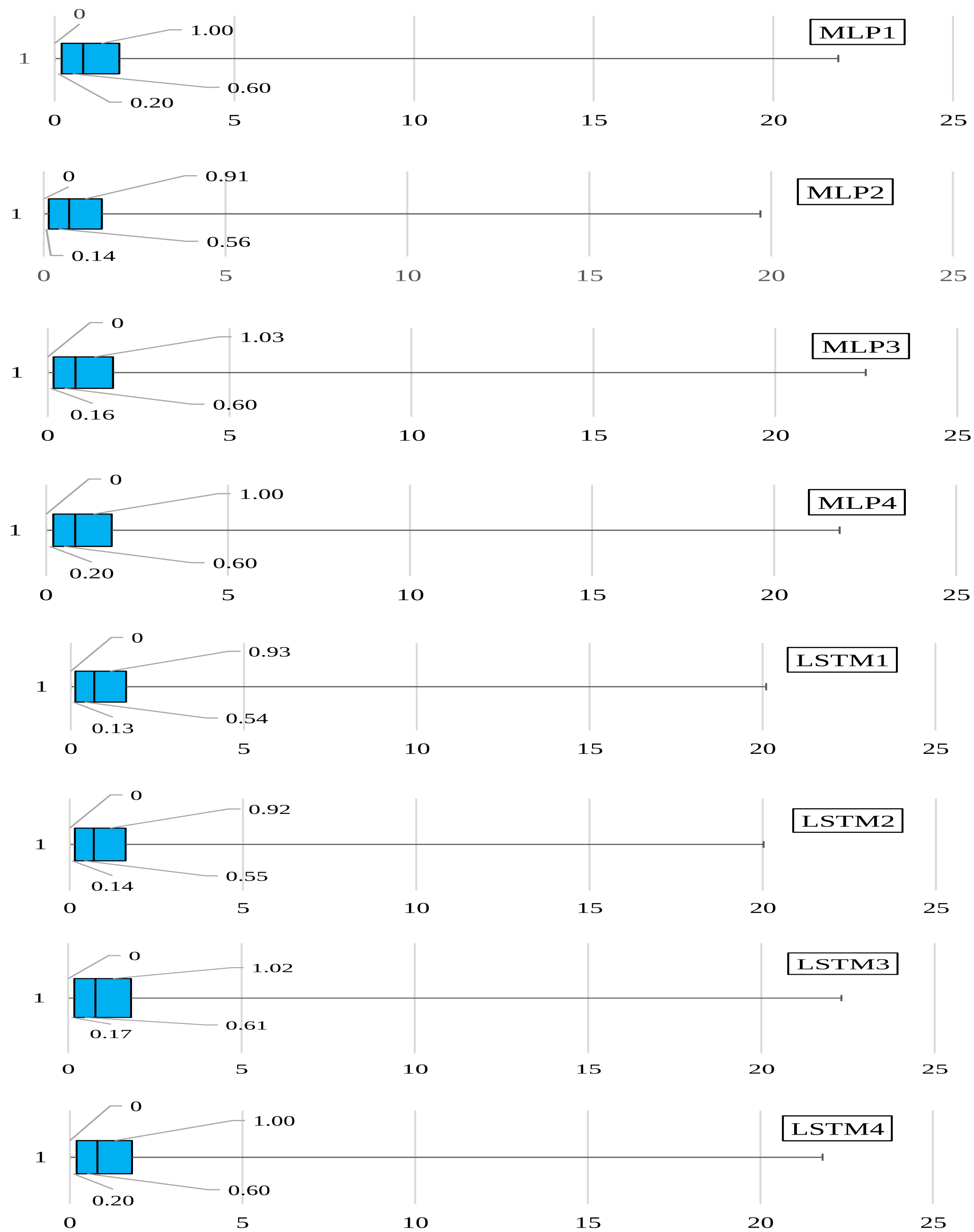

Fig. 11. Box diagram of MLP and LSTM models for Ghramsar station.

Considering LSTM and MLP, Taylor Diagram [58] was drawn to investigate and analyze the values of RMSE, R^2 and standard deviation between the observed evaporation data of Semnan and Garmsar stations with data modeled by LSTM and MLP models (Figure 12). This figure shows that the LSTM4 model is the most accurate prediction model for both studied cities. Also, by comparing the combinations of the MLP model together, the MLP4 model performed better for both cities. It should be noted that this diagram is presented in two forms, semicircle and quadrilateral (only to show positive correlations). In both types, the values of R^2 are plotted as the radius of a circle on its arc, the values of standard deviation are plotted as concentric circles relative to the center of the circle, and the RMSE values are plotted as concentric circles relative to the reference point (solid circle). The results show that the performance of both models is close to each other and acceptable for all scenarios. Gao et al. [74], indicating the better performance of the proposed LSTM model. Chia et al [75], who reported minimum MAE and RMSE values of 0.444 mm/d and 0.543 mm/d, respectively. These results are relatively close to the results of the present study.

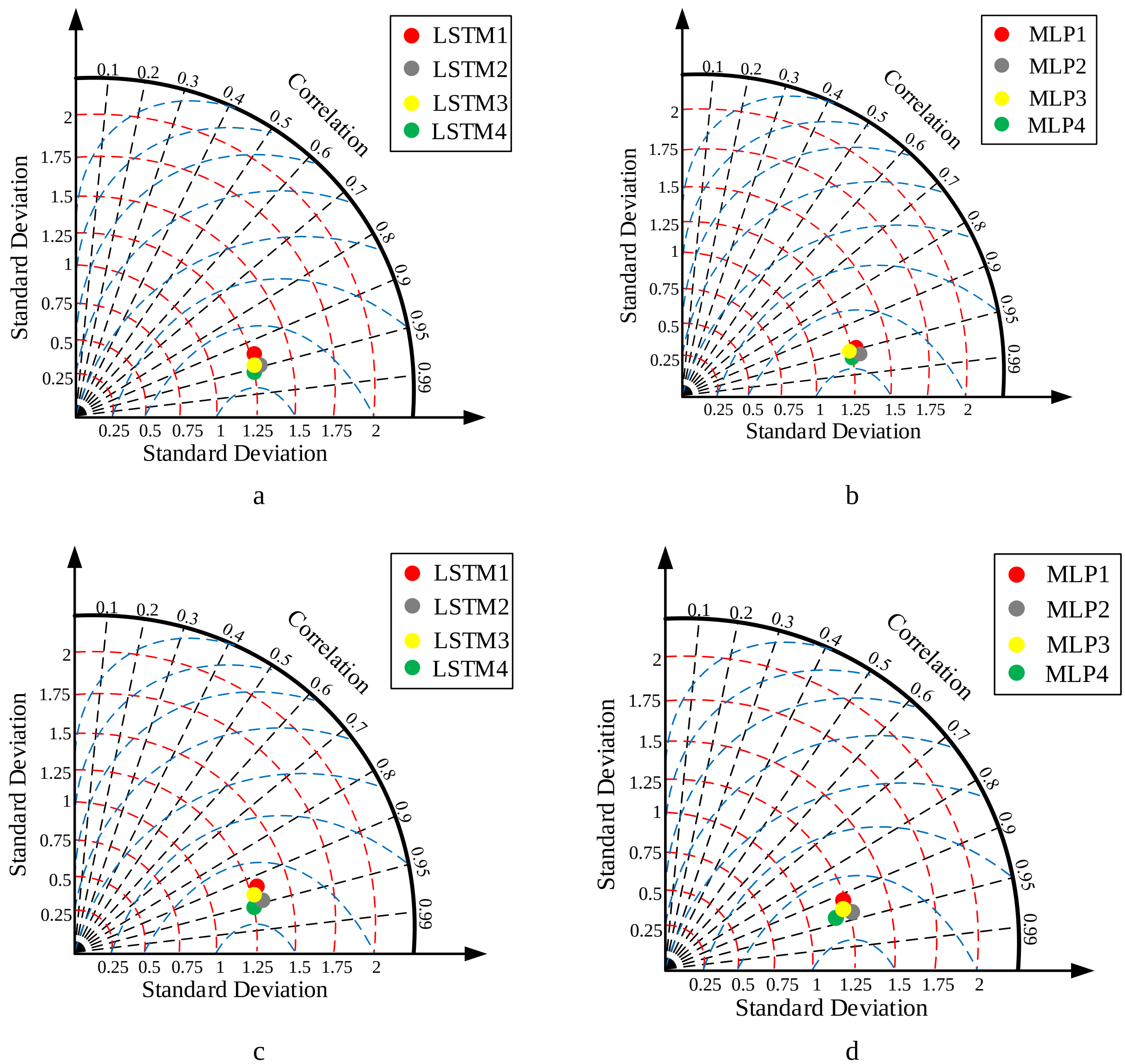

Fig. 12. Taylor diagram for LSTM and MLP models, A and B: Semnan station; C and D: Garmsar station.

7. Conclusion

Soft computational models and statistical techniques are useful frameworks for predicting complex climate indicators, such as pan evaporation. This study was performed to evaluate the potential of Deep-LSTM structure and compare it with MLP to estimate daily evaporation under hot and dry climates with the use of meteorological data. Meteorological parameters used in this research were Minimum and maximum air temperature (Tmax, Tmin), wind speed (WS), sunshine hours (SH), air pressure (PA), relative humidity (RH). In this study 4 input combinations were considered for the two models. Prediction models were tested and trained using daily evaporation data from the existing pan from 2000 to 2018. The accuracy of the models was compared by calculating the statistical criteria of standard R^2, RMSE and MAE.

The following results were obtained in this study:

- LSTM and MLP models can perform well in daily EP simulations.
- The LSTM model performed better in all scenarios than the MLP model.
- Simultaneous consideration of all inputs, in both LSTM and MLP models and for both Semnan and Garmsar stations showed the best performance.
- Due to the availability of methodological data, LSTM can be used as a suitable model for estimating the daily evaporation rate in stations where direct evaporation measurement is not performed.
- Other neural network structures based on deep learning can also be used to predict the process of evaporation from the pan and reference evapotranspiration.

For future research, it is suggested to investigate the LSTM model for different weather conditions. For multi-stage evaporation prediction, LSTM model and other deep learning models such as CNN, Bi LSTM, etc. should be investigated.

Funding

This research received no external funding.

Conflicts of interest

The authors declare no conflict of interest.

Authors contribution statement

AS[1], YD: Conceptualization; HG, HK: Data curation; AS[1], AS[2]: Formal analysis; HK, HA, YD: Investigation; AS[1], HA, AS[2]: Methodology; HK, HR: Project administration; AS[1], YD, HA: Resources; AS[1], HG, AS[2]: Software; HK: Supervision; HK, HG, SA[1], YD, SA[2]: Validation; AS[1], HK: Visualization; HG, AS, YD, HK, AS: Roles/Writing – original draft; HK, AS[1], HG, AS[2], YD: Writing – review & editing.

References

[1] Dadrasajirlou Y, Karami H, Mirjalili S. Using AHP-PROMOTHEE for Selection of Best Low-Impact Development Designs for Urban Flood Mitigation. Water Resour Manag 2023;37:375–402. https://doi.org/10.1007/s11269-022-03378-9.

[2] Ghazvinian H, Karami H. Effect of Rainfall Intensity and Slope at the Beginning of Sandy Loam Soil Runoff using Rain Simulator (Case Study: Semnan City). J Water Soil Sci 2023;26:319–34.

[3] Karami H, Ghazvinian H. A Practical and Economic Assessment Regarding the Effect of Various Physical Covers on Reducing Evaporation from Water Reservoirs in Arid and Semi-Arid Regions (Experimental Study). Iran J Soil Water Res ISNN 2022;53:1297–313.

[4] Salehi S, Niksokhan mohammad H, Ardestani M. Estimating the effects of black porous polyethylene shade covers on evaporation rate in dam reservoirs. Iran J Soil Water Res 2018;49:1017–29. https://doi.org/10.22059/ijswr.2018.236176.667709.

[5] Raziei T, Pereira LS. Estimation of ETo with Hargreaves–Samani and FAO-PM temperature methods for a wide range of climates in Iran. Agric Water Manag 2013;121:1–18.

[6] Dadrasajirlou Y, Ghazvinian H, Heddam S, Ganji M. Reference Evapotranspiration Estimation using ANN, LSSVM, and M5 Tree Models (Case Study: of Babolsar and Ramsar Regions, Iran). J Soft Comput Civ Eng 2022;6:103–21. https://doi.org/10.22115/scce.2022.342290.1434.

[7] Rao MV, Babu VR, Rao LVG, Sastry JS. Estimation of evaporation rates over the Arabian Sea from satellite data. J Earth Syst Sci 1986;95:417–26. https://doi.org/10.1007/BF02842508.

[8] Ghazvinian H, Karami H, Farzin S, Mousavi SF. Experimental Study of Evaporation Reduction Using Polystyrene Coating, Wood and Wax and its Estimation by Intelligent Algorithms. Irrig Water Eng 2020;11:147–65. https://doi.org/10.22125/iwe.2020.120727.

[9] Khobragade SD, Semwal P, Senthil Kumar AR, Nainwal HC. Pan coefficients for estimating open-water surface evaporation for a humid tropical monsoon climate region in India. J Earth Syst Sci 2019;128:175. https://doi.org/10.1007/s12040-019-1198-2.

[10] Ghazvinian H, Farzin S, Karami H, Mousavi SF. Investigating the Effect of using Polystyrene sheets on Evaporation Reduction from Water-storage Reservoirs in Arid and Semiarid Regions (Case study: Semnan city). J Water Sustain Dev 2020;7:45–52. https://doi.org/10.22067/jwsd.v7i2.81748.

[11] Allawi MF, El-Shafie A. Utilizing RBF-NN and ANFIS Methods for Multi-Lead ahead Prediction Model of Evaporation from Reservoir. Water Resour Manag 2016;30:4773–88. https://doi.org/10.1007/s11269-016-1452-1.

[12] Malik A, Kumar A, Kisi O. Daily Pan Evaporation Estimation Using Heuristic Methods with Gamma Test. J Irrig Drain Eng 2018;144:04018023. https://doi.org/10.1061/(ASCE)IR.1943-4774.0001336.

[13] Patle GT, Chettri M, Jhajharia D. Monthly pan evaporation modelling using multiple linear regression and artificial neural network techniques. Water Supply 2020;20:800–8. https://doi.org/10.2166/ws.2019.189.

[14] Qasem SN, Samadianfard S, Kheshtgar S, Jarhan S, Kisi O, Shamshirband S, et al. Modeling monthly pan evaporation using wavelet support vector regression and wavelet artificial neural networks in arid and humid climates. Eng Appl Comput Fluid Mech 2019;13:177–87. https://doi.org/10.1080/19942060.2018.1564702.

[15] Bhalwankar R V., Sathe AB, Kamra AK. The evaporation of the charged and uncharged water drops suspended in a wind tunnel. J Earth Syst Sci 2004;113:129–38. https://doi.org/10.1007/BF02709783.

[16] Irmak S, Haman DZ, Jones JW. Evaluation of Class A Pan Coefficients for Estimating Reference Evapotranspiration in Humid Location. J Irrig Drain Eng 2002;128:153–9. https://doi.org/10.1061/(ASCE)0733-9437(2002)128:3(153).

[17] Ghazvinian H, Karami H, Farzin S, Mousavi S-F. Introducing affordable and accessible physical covers to reduce evaporation from agricultural water reservoirs and pools (field study, statistics, and intelligent methods). Arab J Geosci 2021;14:2543. https://doi.org/10.1007/s12517-021-08735-3.

[18] Abiye OE, Matthew OJ, Sunmonu LA, Babatunde OA. Potential evapotranspiration trends in West Africa from 1906 to 2015. SN Appl Sci 2019;1:1434. https://doi.org/10.1007/s42452-019-1456-6.

[19] Ndiaye PM, Bodian A, Diop L, Deme A, Dezetter A, Djaman K, et al. Trend and Sensitivity Analysis of Reference Evapotranspiration in the Senegal River Basin Using NASA Meteorological Data. Water 2020;12:1957. https://doi.org/10.3390/w12071957.

[20] Nourani V, Sayyah Fard M. Sensitivity analysis of the artificial neural network outputs in simulation of the evaporation process at different climatologic regimes. Adv Eng Softw 2012;47:127–46. https://doi.org/10.1016/j.advengsoft.2011.12.014.

[21] Singh A, Singh RM, Kumar ARS, Kumar A, Hanwat S, Tripathi VK. Evaluation of soft computing and regression-based techniques for the estimation of evaporation. J Water Clim Chang 2021;12:32–43. https://doi.org/10.2166/wcc.2019.101.

[22] SINGH VP, XU C-Y. Evaluation and Generalization of 13 Mass-Transfer Equations for Determining Free Water Evaporation. Hydrol Process 1997;11:311–23. https://doi.org/10.1002/(SICI)1099-1085(19970315)11:3<311::AID-HYP446>3.0.CO;2-Y.

[23] Adnan RM, Malik A, Kumar A, Parmar KS, Kisi O. Pan evaporation modeling by three different neuro-fuzzy intelligent systems using climatic inputs. Arab J Geosci 2019;12:606. https://doi.org/10.1007/s12517-019-4781-6.

[24] Ghazvinian H, Karami H, Farzin S, Mousavi SF. Effect of MDF-Cover for Water Reservoir Evaporation Reduction, Experimental, and Soft Computing Approaches. J Soft Comput Civ Eng 2020;4:98–110. https://doi.org/10.22115/scce.2020.213617.1156.

[25] Keshtegar B, Heddam S, Sebbar A, Zhu S-P, Trung N-T. SVR-RSM: a hybrid heuristic method for modeling monthly pan evaporation. Environ Sci Pollut Res 2019;26:35807–26. https://doi.org/10.1007/s11356-019-06596-8.

[26] Shabani S, Samadianfard S, Sattari MT, Mosavi A, Shamshirband S, Kmet T, et al. Modeling Pan Evaporation Using Gaussian Process Regression K-Nearest Neighbors Random Forest and Support Vector Machines; Comparative Analysis. Atmosphere (Basel) 2020;11:66. https://doi.org/10.3390/atmos11010066.

[27] Kumar M, Raghuwanshi NS, Singh R, Wallender WW, Pruitt WO. Estimating Evapotranspiration using Artificial Neural Network. J Irrig Drain Eng 2002;128:224–33. https://doi.org/10.1061/(ASCE)0733-9437(2002)128:4(224).

[28] Moghaddamnia A, Ghafari Gousheh M, Piri J, Amin S, Han D. Evaporation estimation using artificial neural networks and adaptive neuro-fuzzy inference system techniques. Adv Water Resour 2009;32:88–97. https://doi.org/10.1016/j.advwatres.2008.10.005.

[29] Ashrafzadeh A, Malik A, Jothiprakash V, Ghorbani MA, Biazar SM. Estimation of daily pan evaporation using neural networks and meta-heuristic approaches. ISH J Hydraul Eng 2020;26:421–9. https://doi.org/10.1080/09715010.2018.1498754.

[30] Ghorbani K, Aligholinia T, Rasouli Majd N. Accuracy Evaluation of Twenty Empirical Models in Estimating Coastal Regions Reference Evapotranspiration in different climate. J Water Soil Conserv 2018;25:307–20. https://doi.org/10.22069/jwsc.2018.14411.2917.

[31] Dehghanipour MH, Karami H, Ghazvinian H, Kalantari Z, Dehghanipour AH. Two comprehensive and practical methods for simulating pan evaporation under different climatic conditions in iran. Water (Switzerland) 2021;13:2814. https://doi.org/10.3390/w13202814.

[32] Aghelpour P, Mohammadi B, Biazar SM. Long-term monthly average temperature forecasting in some climate types of Iran, using the models SARIMA, SVR, and SVR-FA. Theor Appl Climatol 2019;138:1471–80.

[33] Moazenzadeh R, Mohammadi B, Shamshirband S, Chau K. Coupling a firefly algorithm with support vector regression to predict evaporation in northern Iran. Eng Appl Comput Fluid Mech 2018;12:584–97. https://doi.org/10.1080/19942060.2018.1482476.

[34] Shabani S, Samadianfard S, Sattari MT, Shamshirband S, Mosavi A, Kmet T, et al. Modeling daily pan evaporation in humid climates using gaussian process regression. ArXiv Prepr ArXiv190804267 2019.

[35] Emadi A, Zamanzad-Ghavidel S, Fazeli S, Zarei S, Rashid-Niaghi A. Multivariate modeling of pan evaporation in monthly temporal resolution using a hybrid evolutionary data-driven method (case study: Urmia Lake and Gavkhouni basins). Environ Monit Assess 2021;193:1–32.

[36] Malik A, Kumar A, Kim S, Kashani MH, Karimi V, Sharafati A, et al. Modeling monthly pan evaporation process over the Indian central Himalayas: application of multiple learning artificial intelligence model. Eng Appl Comput Fluid Mech 2020;14:323–38.

[37] Sattari MT, Ahmadifar V, Delirhasannia R, Apaydín H. Estimation of the pan evaporation coefficient in cold and dry climate conditions via the M5 regression tree model. Atmósfera 2021;34:289–300.

[38] Wang L, Kisi O, Hu B, Bilal M, Zounemat-Kermani M, Li H. Evaporation modelling using different machine learning techniques. Int J Climatol 2017;37:1076–92. https://doi.org/10.1002/joc.5064.

[39] Abbas MY. Estimating daily evaporation in syrian coast using gene expression programming and adaptive neuro-fuzzy inference system. J Eng Comput Sci 2020;21:48–55.

[40] Izady A, Sanikhani H, Abdalla O, Chen M, Kisi O. Impurity effect on clear water evaporation: toward modelling wastewater evaporation using ANN, ANFIS-SC and GEP techniques. Hydrol Sci J 2017;62:1856–66.

[41] Arya Azar N, Ghordoyee Milan S, Kayhomayoon Z. Predicting monthly evaporation from dam reservoirs using LS-SVR and ANFIS optimized by Harris hawks optimization algorithm. Environ Monit Assess 2021;193:1–14.

[42] Keshtegar B, Kisi O. Modified Response-Surface Method: New Approach for Modeling Pan Evaporation. J Hydrol Eng 2017;22:04017045. https://doi.org/10.1061/(ASCE)HE.1943-5584.0001541.

[43] Zounemat-Kermani M, Kisi O, Piri J, Mahdavi-Meymand A. Assessment of Artificial Intelligence–Based Models and Metaheuristic Algorithms in Modeling Evaporation. J Hydrol Eng 2019;24:04019033. https://doi.org/10.1061/(ASCE)HE.1943-5584.0001835.

[44] Tikhamarine Y, Malik A, Pandey K, Sammen SS, Souag-Gamane D, Heddam S, et al. Monthly evapotranspiration estimation using optimal climatic parameters: efficacy of hybrid support vector regression integrated with whale optimization algorithm. Environ Monit Assess 2020;192:696. https://doi.org/10.1007/s10661-020-08659-7.

[45] Yaseen ZM, Ebtehaj I, Bonakdari H, Deo RC, Mehr AD, Mohtar WHMW, et al. Novel approach for streamflow forecasting using a hybrid ANFIS-FFA model. J Hydrol 2017;554:263–76.

[46] Zounemat-Kermani M, Keshtegar B, Kisi O, Scholz M. Towards a Comprehensive Assessment of Statistical versus Soft Computing Models in Hydrology: Application to Monthly Pan Evaporation Prediction. Water 2021;13:2451. https://doi.org/10.3390/w13172451.

[47] Ghazvinian H, Bahrami H, Ghazvinian H, Heddam S. Simulation of Monthly Precipitation in Semnan City Using ANN Artificial Intelligence Model. J Soft Comput Civ Eng 2020;4:36–46. https://doi.org/10.22115/scce.2020.242813.1251.

[48] Koohbanani H, Yazdani M. Mapping the Moisture of Surface Soil Using Landsat 8 Imagery (Case study: Suburb of Semnan City). Geogr Sustain Environ 2018;8:65–77.

[49] Kisi O. Pan evaporation modeling using least square support vector machine, multivariate adaptive regression splines and M5 model tree. J Hydrol 2015;528:312–20. https://doi.org/10.1016/j.jhydrol.2015.06.052.

[50] Malik A, Kumar A, Kisi O. Monthly pan-evaporation estimation in Indian central Himalayas using different heuristic approaches and climate based models. Comput Electron Agric 2017;143:302–13. https://doi.org/10.1016/j.compag.2017.11.008.

[51] Eray O, Mert C, Kisi O. Comparison of multi-gene genetic programming and dynamic evolving neural-fuzzy inference system in modeling pan evaporation. Hydrol Res 2018;49:1221–33. https://doi.org/10.2166/nh.2017.076.

[52] Majhi B, Naidu D, Mishra AP, Satapathy SC. Improved prediction of daily pan evaporation using Deep-LSTM model. Neural Comput Appl 2020;32:7823–38. https://doi.org/10.1007/s00521-019-04127-7.

[53] Karami H, Ghazvinian H, Dehghanipour M, Ferdosian M. Investigating the Performance of Neural Network Based Group Method of Data Handling to Pan's Daily Evaporation Estimation (Case Study: Garmsar City). J Soft Comput Civ Eng 2021;5:1–18. https://doi.org/10.22115/scce.2021.274484.1282.

[54] Shahi S, Mousavi SF, Hosseini K. Simulation of Pan Evaporation Rate by ANN Artificial Intelligence Model in Damghan Region. J Soft Comput Civ Eng 2021;5:75–87. https://doi.org/10.22115/scce.2021.286933.1321.

[55] Abed M, Imteaz MA, Ahmed AN, Huang YF. Application of long short-term memory neural network technique for predicting monthly pan evaporation. Sci Rep 2021;11:1–19.

[56] Roy DK, Sarkar TK, Kamar SSA, Goswami T, Muktadir MA, Al-Ghobari HM, et al. Daily Prediction and Multi-Step Forward Forecasting of Reference Evapotranspiration Using LSTM and Bi-LSTM Models. Agronomy 2022;12:594. https://doi.org/10.3390/agronomy12030594.

[57] Sandberg IW, Lo JT, Fancourt CL, Principe JC, Katagiri S, Haykin S. Nonlinear dynamical systems: feedforward neural network perspectives. vol. 21. John Wiley & Sons; 2001.

[58] Taylor KE. Summarizing multiple aspects of model performance in a single diagram. J Geophys Res Atmos 2001;106:7183–92. https://doi.org/10.1029/2000JD900719.

[59] Fakharian P, Rezazadeh Eidgahee D, Akbari M, Jahangir H, Ali Taeb A. Compressive strength prediction of hollow concrete masonry blocks using artificial intelligence algorithms. Structures 2023;47:1790–802. https://doi.org/10.1016/j.istruc.2022.12.007.

[60] Naderpour H, Sharei M, Fakharian P, Heravi MA. Shear Strength Prediction of Reinforced Concrete Shear Wall Using ANN, GMDH-NN and GEP. J Soft Comput Civ Eng 2022;6:66–87. https://doi.org/10.22115/scce.2022.283486.1308.

[61] Fausett L V. Fundamentals of neural networks: architectures, algorithms and applications. Pearson Education India; 2006.

[62] Hochreiter S, Schmidhuber J. Long short-term memory. Neural Comput 1997;9:1735–80.

[63] Graves A. Generating sequences with recurrent neural networks. ArXiv Prepr ArXiv13080850 2013.

[64] Hu Z, Karami H, Rezaei A, DadrasAjirlou Y, Piran MJ, Band SS, et al. Using soft computing and machine learning algorithms to predict the discharge coefficient of curved labyrinth overflows. Eng Appl Comput Fluid Mech 2021;15:1002–15. https://doi.org/10.1080/19942060.2021.1934546.

[65] Ghanizadeh AR, Ghanizadeh A, Asteris PG, Fakharian P, Armaghani DJ. Developing bearing capacity model for geogrid-reinforced stone columns improved soft clay utilizing MARS-EBS hybrid method. Transp Geotech 2023;38:100906. https://doi.org/10.1016/j.trgeo.2022.100906.

[66] Karami H, DadrasAjirlou Y, Jun C, Bateni SM, Band SS, Mosavi A, et al. A Novel Approach for Estimation of Sediment Load in Dam Reservoir With Hybrid Intelligent Algorithms. Front Environ Sci 2022;10. https://doi.org/10.3389/fenvs.2022.821079.

[67] Eftekhari M, Eslaminezhad SA, Akbari M, DadrasAjirlou Y, Haji Elyasi A. Assessment of the Potential of Groundwater Quality Indicators by Geostatistical Methods in Semi-arid Regions. J

Chinese Soil Water Conserv 2021;52:158–67. https://doi.org/10.29417/JCSWC.202109_52(3).0004.

[68] Ghazvinian H, Mousavi S-F, Karami H, Farzin S, Ehteram M, Hossain MS, et al. Integrated support vector regression and an improved particle swarm optimization-based model for solar radiation prediction. PLoS One 2019;14:e0217634. https://doi.org/10.1371/journal.pone.0217634.

[69] Wang L, Kisi O, Zounemat-Kermani M, Li H. Pan evaporation modeling using six different heuristic computing methods in different climates of China. J Hydrol 2017;544:407–27. https://doi.org/10.1016/j.jhydrol.2016.11.059.

[70] Fan J, Wu L, Zhang F, Xiang Y, Zheng J. Climate change effects on reference crop evapotranspiration across different climatic zones of China during 1956–2015. J Hydrol 2016;542:923–37.

[71] Alsumaiei AA. Utility of Artificial Neural Networks in Modeling Pan Evaporation in Hyper-Arid Climates. Water 2020;12:1508. https://doi.org/10.3390/w12051508.

[72] Yin J, Deng Z, Ines AVM, Wu J, Rasu E. Forecast of short-term daily reference evapotranspiration under limited meteorological variables using a hybrid bi-directional long short-term memory model (Bi-LSTM). Agric Water Manag 2020;242:106386.

[73] Ferreira LB, da Cunha FF. Multi-step ahead forecasting of daily reference evapotranspiration using deep learning. Comput Electron Agric 2020;178:105728.

[74] Gao L, Gong D, Cui N, Lv M, Feng Y. Evaluation of bio-inspired optimization algorithms hybrid with artificial neural network for reference crop evapotranspiration estimation. Comput Electron Agric 2021;190:106466. https://doi.org/10.1016/j.compag.2021.106466.

[75] Chia MY, Huang YF, Koo CH. Resolving data-hungry nature of machine learning reference evapotranspiration estimating models using inter-model ensembles with various data management schemes. Agric Water Manag 2022;261:107343.